Journal of the European Ceramic Society **18** (1998) 1339–1350

PII: S0955-2219(98)00063-6
0955-2219/98/$—see front matter

Ceramic Foams by Powder Processing

L. Montanaro,[a]* Y. Jorand,[b] G. Fantozzi[b] and A. Negro[a]

[a]Department of Materials Sciences and Chemical Engineering, Politecnico, Cso. Duca degli Abruzzi 24, 10129 Torino, Italy
[b]G.E.M.P.P.M., U.M.R. 5510, I.N.S.A Lyon, Bat. 502, 69621 Villeurbanne cedex, France

Abstract

Ceramic foams show a significant potential of development and application, essentially due to the emergence of environmental preoccupations. A brief overview of the state of the art in cellular ceramic application, preparation and characterization is presented in order to introduce some new data concerning the elaboration of mullite and PZT foams by a replication and a bubble generation method, respectively. Some discrepancies between the theory, developed for describing the properties of open-cell foams, and the experimental mechanical behaviour of these semi-closed cell materials were also shown.

1 Introduction

The objective of this paper is to present an overview of the state of the art, to give new data concerning the elaboration of porous materials and comparing them to the literature.

Introducing cellular solids, Ashby[1] considered that when man builds large load-bearing structures, he uses dense solids: steel, concrete, glass. When nature does the same, she generally uses cellular materials: wood, bone, coral. It is almost certainly that cellular materials permit the simultaneous optimization of stiffness, strength and overall weight in a given application.

Cellular ceramics are comprised of various arrangements of a space-filling polygons (cells) and can be classified into two broad groups: honeycombs and foams.[2]

In honeycomb the cells form a two-dimensional array, whereas foams are comprised of a three-dimensional array of hollow polygons. Foams are usually sub-divided into two further categories, depending on whether or not the individual cells possess solid faces.

*To whom correspondence should be addressed. Fax: 00391-11-564-46-65; e-mail: negro@athena.polito.it

If the solid of which the foam is made is contained only in cell edges, the material is termed open-cell. If the cell faces are present, the foam is termed closed-cell and the individual cells are isolated from each other.

There is clearly the possibility that foams can be partly open and partly closed.

These porous network structures[3] have relatively low mass, low density, and low thermal conductivity, and differ in the property of permeability, having the open-pore ones the higher permeability. By combining the proper ceramic materials and processing, porous ceramics can also have relatively high strength, high resistance to chemical attack, high temperature resistance, high structural uniformity.

2 Present and Future Applications

These properties make ceramic foams suitable for a variety of applications. Both closed-cell and open-cell foams are used as thermal insulating materials for furnaces and also for aerospace applications (tiles for space shuttles), fire protection materials, low mass kiln furniture and gas combustion burners. The most common applications for open-cell porous ceramics are molten metal and Diesel engine exhaust filters, catalyst supports,[4] industrial hot gas filters, grease filter for commercial kitchens.[5] Expanding applications are now also being found in the electronic and biomedical areas. The foams already commercially available or in study are made of various materials, following the constraints of specific applications, as cordierite;[4,6] mullite;[1,7,8] silicon carbide;[2,9] alumina;[2,8–12] partially stabilized zirconia;[1,8,9,12] and some composite systems (SiC–alumina;[13] alumina–zirconia;[2] alumina–mullite;[2] mullite–zirconia).

2.1 Thermal insulation

A principal application of these foams is in fabrication of thermal insulators, due to their specific characteristics, as thermal stability, low thermal

conductivity, low density, resistance to thermal cycling, thermal shock resistance, low gas adsorption and absorption, low specific heat, and also because they are available in various size and configurations.

Preliminary measurements of a zirconia foam reveal that thermal insulation equivalent to that of NASA space shuttle protective thermal tiles can be achieved at 550°C higher operating temperature.

Many different compositions of refractory foams were investigated (carbon, oxide and non-oxide materials).[12,14]

2.2 Molten metal filtration

For production of castings, foam ceramic filters are helping to improve quality and productivity by removing non metallic inclusions; the filters must be able to resist attack at high temperatures by a variety of molten metals, which can contain such reactive elements as aluminium, titanium, hafnium and carbon. Thermal shock behaviour is obviously also important: it was found to be strongly dependent on cell size (increasing with increasing cell size) and weakly dependent on density (increasing with increasing density).

The material selected depends on the material to be filtered and is usually a metallic oxide of various compositions (Table 1).[8,15]

2.3 Hot gas cleanup

Application of high-performance, high-temperature particulate control ceramic filters is expected to be beneficial not only to the advanced fossil-fuel processing technologies, but also to high-temperature industrial processes, waste incineration processes and to diesel soot filtration. Development and utilization of hot gas filtration depends on the creatice design and use of new high-temperature materials.

The criteria for successful use and operation of porous filters as a viable advanced particulate removal concept therefore requires not only thermal, chemical and mechanical stability of ceramic materials, but also long-term structural durability ($> 10\,000$ h) of the entire filter and high reliability of integrated process design features.[16,17]

Such filters must withstand variation in the effluent gas stream chemistry, variation in the nature and loadings of the entrained fines, and oscillations in the effluent gas stream temperature and possible pressure, while still maintaining high particulate removal efficiencies, high flow capacity, and relatively low pressure drop flow characteristics. During operation the filter must also withstand a variety of mechanical, vibration, and thermal stresses.

The principal materials for these applications include alumina, mullite, cordierite, silicon nitride, silicon carbide. Both alumina/mullite and cordierite have been demonstrated to have certain advantages over non-oxide materials. The oxides already contain stable oxide phases which do not undergo further phase transition. They also retain their physical integrity during exposure to gas phase alkali: in fact long-term degradation mechanisms may result from chemical reactions, particularly with alkali species and/or steam, which would affect the long-term durability of the system.

Even if till now candle filters and cross-flow filters have been mainly applied, ceramic foams are presently investigated, above all for diesel soot filtration, for their high particulate removal efficiency, their high flow capacity and low pressure drop generation.[6,10,18]

3 Processing

Numerous processing routes are available to realize porous ceramics:[15] capsule-free HIP, bubbles generation into a slurry or at a green state during a specific thermal treatment, reaction sintering, control of the sintering conditions in order to achieve a partial densification, stacking of presintered granules or fibres, aerogel and sol–gel methods, pyrolysis of various organic additives, polymeric sponge method.

Table 1. Some characteristics of molten metal filters

Tradename	*Composition*	*Applications*	*Benefits*
Celtrex	55% Al_2O_3. 38%SiO_2·7%MgO	Iron alloys	Reduction in scrap rate
Corning	77% Al_2O_3. 23% SiO_2	Carbon low alloy, stainless steel	Pouring temperatures up to 1675°C
Cerapor	Alumina, SiC, cordierite, ZrO_2	Aluminum, iron, copper, bronze, steel, zinc	Laminated duplex and triplex construction
Udicell	Alumina, mullite, ZTA, PSZ	Superalloys, low-carbon stainless steel	Large volumes up to 120 tons
Alucel	92% alumina with mullite phase	Nonferrous alloys	Improved thermal shock resistance, smaller filters required
Selee	Alumina, PSZ	Aluminum, iron, steel	High flow rates

This paper deals on the foam ceramics processed by:

- a replication method or polymeric sponge method;
- bubble generation method by a pore foaming agent.

3.1 Polymeric sponge method

The first method, patented in 1963,[19] consists in the impregnation of a polymeric sponge with a ceramic slurry followed by a thermal treatment which leads to the burning out of the organic portion and to the sintering of the ceramic skeleton.

Many steps must be optimized to develop a foam product having the desired performances, namely: the choice of the polymeric template; the preparation of the ceramic slurry; the impregnation; the thermal cycle comprising drying, burning out of the volative components, sintering of the ceramic portion.

A variety of open-cell, semi-closed and closed-cell sponge materials are suited to replication process; their pore size determines the pore size of the ceramic foam after the shrinkage linked to the firing step.

The sponge should volatilize at low temperature without yielding noxious by-products; in addition, it must readily soften and burn off, without inducing sensible residual stresses and disrupting the unsintered ceramic network. Its resiliency, its hydrophobic behaviour and its ability to be uniformly covered are other significant properties.

Many polymeric-sponge materials can satisfy these requirements, namely poly(urethane), cellulose, poly(vinyl chloride), poly(styrene), latex. In some cases, spongelike polymers (like polysilanes, polycarbosilanes) have been used to prepare silicon carbide foams by pyrolysis: these pyrolyzed porous networks were then immersed in ceramic (α-alumina) slurries to obtain a composite foam.[13]

One of the key steps of this process is undoubtedly the elaboration of an appropriate ceramic slurry able to uniformly cover the polymeric walls, to easily sinter in a dense ceramic network, able to withstand the in-use constraints.

Even if limited information can be found in literature, being a large number of foam elaboration processes patented, it is certain that a common slurry for this application is formed by a ceramic powder, a dispersion medium (generally water) and some additives. Two typical slurry formulations, respectively in aqueous and non-aqueous medium, are reported in Tables 2 and 3.[3] The ceramic material is firstly obviously chosen depending on the particular application and desired properties of the final foam.

A pure, fine ceramic powder having a narrow particle size distribution is usually requested: dimensions lower than 45 micron are common, and generally the mean particle size is close to few microns. In addition, equiaxial particles should lead to a more homogeneous coating of the polymeric walls.

Table 2. Polymeric sponge process: typical aqueous based recipe[3]

1. Prepare ceramic slurry	
Al_2O_3	47% by weight
Cr_2O_3	13%
Kaolin	3·5%
Bentonite	1%
Colloidal aluminium orthophospahte in water	14·5%
Water	
for a total slurry content of 82% solids, 18% water	
2 Immerse 5 cm thick poly(urethane) foam in ceramic slurry.	
3. Knead foam to remove excess air; remove from slurry.	
4. Pass impregnated foam through rollers to remove 80% of slurry.	
5. Oven dry at 125°C for 1 h.	
6. Slowly heat at 0·5°C min^{-1} to 500°C; hold at 500°C for 1 h	
7. Heat to 1350°C at 1°C min^{-1} and hold for 5 h	
Final properties	
Permeability	1425×10^{-7} cm^2
Porosity	0·87
Pore size	12 pores/linear cm^{-1}
Thickness	5 cm
Structural uniformity	Excellent

The quantity of particles that can enter a sponge depends on factors which are related to the structure of the sponge (that is its suction force, which is optimized increasing the open porosity of the sponge, and its ability to retain the ceramic particles, against gravity force), but also to the concentration of the slurry.

The slurries contain very variable solid weight percent, but usually ranging between 50 and 70 wt% of solids. For higher solid concentrations, the slurry becomes more and more viscous and the particles might then have difficulty in entering the sponge structure: therefore, the sponge loading decreases (Fig. 1, Ref. 20).

Many additives should be used for improving the coating performances or even the final sintered foam properties.

Table 3. Polymeric sponge process: nonaqueous slurry composition[3]

Alumina (RC-HPT)	47·5%
90 trichloroethane—10 ethanol	47·5%
Binder (Butvar B—76)	1·9%
Plasticizer (Carbowax PEG—300)	1·0%
Plasticizer (Ucon 50—HB—2000)	1·9%
Dispersant (Sarkosyl O)	0·1%
MgO	0·2%

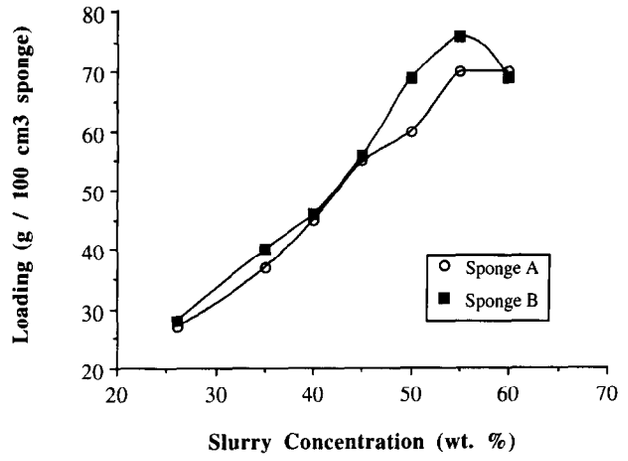

Fig. 1. Relationship between particle loading and slurry concentration.

A binder can provide strength to the ceramic structure after drying and prevent collapse during volatization of the organic portion. Some rheological agent should be added to adjust the slurry viscosity Sometimes a thixotropic behaviour has been suggested for an appropriate coating: when the polymeric sponge is impregnated, the slurry must be fluid enough to enter, fill and uniformly coat the sponge network and subsequently regain enough viscosity under static conditions to remain in the sponge.

In addition, being the impregnation generally conducted by compression to remove air, immersion of the sponge in the slurry, and free expansion of the polymer in the ceramic suspension, it should be supposed that a high viscosity of the slurry retards the movement of the sponge when it tries to recover its original shape.

Different slurry formulations and optimal viscosities are reported in literature. In the case of the coating of a poly(urethane) sponge by a pottery clay slurry, containing sodium carbonate—41 wt% related to clay—as defloculant, the evolution of the viscosity as a function of slurry concentration is reported in Table 4.[20] They noted a sharp increase in viscosity for slurry concentrations higher than 45 wt% and they concluded that a too much viscous slurry is detrimental to the formation of uniform products. In conclusion, they assume very low viscosity value (about 10–20 mPa s) as the optimum value.

On the contrary, always for the coating of a poly(urethane) sponge by an alpha alumina slurry, slurry concentrations ranging between 60 and 70 wt% in solid were prepared, adding different additives, as clay, calcium and zinc salts. In this case, the viscosity range is very different, as shown in Figs 2 and 3.[11] The clay additions lead to a newtonian behaviour; deviations from the linear behaviours versus time were observed starting from 6 wt% additions, due to the swelling of the clay in water. The calcium and zinc additions lead to a thixotropic behaviour and to limit viscosities higher than in the case of clay (300–600 mPa s against 100–200 mPa s). But, unfortunately the authors do not give the influence of these viscosity parameters on the coating performances. The only data which are indirectly correlated are the

Table 4. Slurry concentration and viscosity

Slurry concentration (wt%)	*Viscosity (cPs.)*
26	1·9
35	2·0
40	4·8
45	12·5
50	1290·0

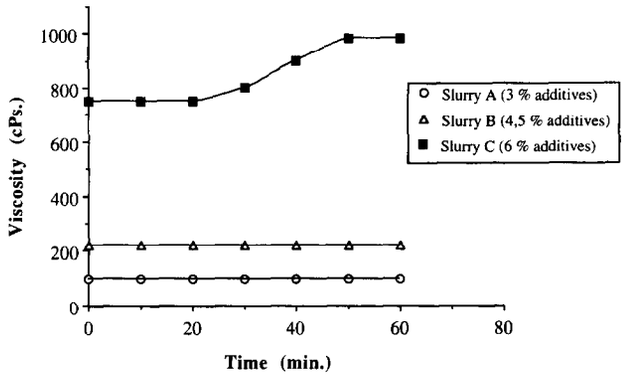

Fig. 2. Viscosity versus time curve for alumina clay slurries.

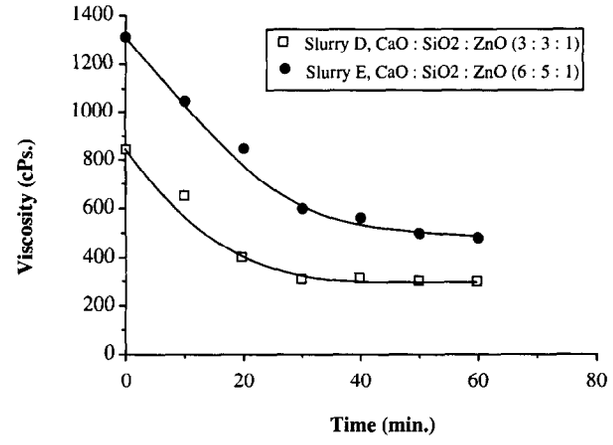

Fig. 3. Viscosity versus time curves for alumina slurries containing CaO, ZnO and SiO_2.

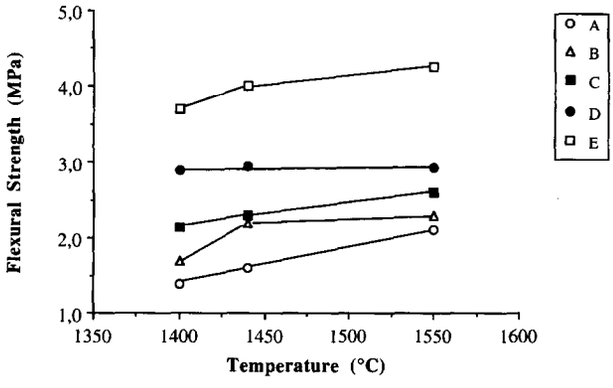

Fig. 4. Mechanical strength versus temperature for alumina foams.

modules of rupture of the foams differently added (Fig. 4, Ref. 11). In another paper,[12] the beneficial effect of polyethylene oxide (PEO, average molecular weight = 100 000) on the coherent and homegeneous coating of a poly(urethane) foam has been underlined. The optimum slurry formulation consists of 40 vol% of ceramic powder (alumina or alumina/zirconia), 2 wt% of a polyelectrolyte (Darvan C) and 1 wt% PEO (referenced to the powder weight in slurry). However, also in this case, the influence of this addition on slurry viscosity was not reported.

Tulliani[7,21] investigated the formulation of mullite slurries for coating poly(urethane) foams in the p.p.i. range 25–65. The aqueous slurries were stabilized at pH 10 by NaOH addition. Different solid concentrations and additives were tested in order to optimize the coating. The viscosity changes were also evaluated. The more significant results are reported in Table 5. The polymeric foams are then immersed in the well dispersed slurries and are compressed whilst submerged in order to fill all the pores. The impregnated poly(urethane) support is then removed from the slurry and excess material squeezed from the foams by means of a rolling mill. Different compression ratios can be set on the mill in order to achieve a well distributed coating on the sponge support and to improve the permeability of the sample. Drying can be done in air or in an oven.

Firing of the samples is a two stage process as shown schematically in Fig. 5.[7] The first stage at about 300°C consists of slowly decomposing and burning out the poly(urethane) support without collapsing the deposited mullite powder, whereas the second stage, at high temperature (1550°C in the mullite case) is for the sintering and densification of the ceramic powder.

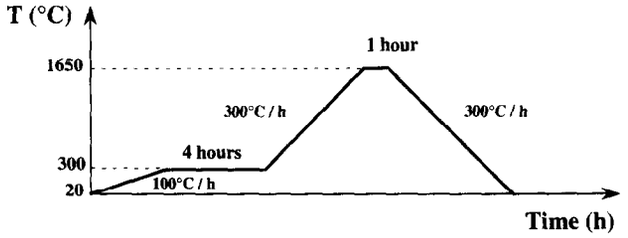

Fig. 5. Thermal cycle for pyrolysis of the organic support and sintering of ceramic coating made of mullite.

Some other thermal cycles reported in literature are the following: for alumina and alumina-zirconia foams[12] the heating schedule consists of a heating rate of 1°C min^{-1} to 550°C, rapid heating (2 h) from 550 to 1600°C and 1 h hold at 1600°C. For alumina foams[11] the samples were heated up to 500°C at 1°C min^{-1}; subsequently, the temperature was raised to 1400–1500°C in 5–8 h. At the final temperature, the material was soaked for 4–8 h and allowed to cool in the furnace. For SiC–alumina foams,[13] the samples were sintered for 1 h at 1300°C in flowing argon and 1 h at 1600°C in 1·5 MPa argon, at a heating rate of 10°C min^{-1}.

The struts and pore walls consist of well sintered material, with a grain size of few microns (Fig. 6.[21]). Some typical defects in microstructure of the foams should be easily observed, as the triangular voids inside struts and long cracks between walls (Fig. 7.[21]). Mercury porosimetry (Fig. 8., Ref. 21) confirms that the pore walls and struts are well densified: there is also a clear indication of a polymodal distribution of the pore sizes. The larger size range is undoubtedly related to the voids inside the struts and between the pore walls whereas the smaller is indicative of the finer porosity within the sintered walls.

Table 5. Composition, viscosity and coating performance of some mullite slurries

Solid concentration (mullite, wt%)	*Additive (wt% referred to mullite)*	*Viscosity (mPa s) (at 20 s^{-1}, at 20°C)*	*Coating*
70	Polyelectrolyte (Darvan C) = 2	150 Newtonian	Bad, discontinuities
70	Polyelectrolyte (Darvan C) = 2 Surfactant (silicone-type) = 1	520 Newtonian	Bad, discontinuities
50	Polyelectrolyte (Darvan C) = 2 Rheological agent (carboxymethylcellulose) = 0·8	1500 slightly thixotropic	Slightly better than the previous coatings
50	Polyelectrolyte (Darvan C) = 2 Rheological agent (carboxymethylcellulose) = 1·6	6300 slightly thixotropic	Slightly better than the previous coating
55	Polyelectrolyte (Darvan C) = 2 Rheological agent (carboxymethylcellulose) = 1·5	8300 thixotropic	Slightly better than the previous coating, but difficulties in homogeneously coating foams having a p.p.i. number higher than 50
60	Polyelectrolyte (Darvan C) = 2 Rheological agent (carboxymethylcellulose) = 1·0	8600 thixotropic	Good coating for foams having a p.p.i. number lower than 50
60	Polyelectrolyte (Darvan C) = 2 Rheological agent (Polyethylene oxide, M.W. = 100 000) = 1·0	130 pseudo-plastic	Good coating for foams having a p.p.i. number higher than 50

3.2 Bubble generation method

The first technique using this method was patented in 1973:[22] in the majority of cases, a chemical mixture containing the desired constituents is treated to evolve a gas which creates bubbles and causes the material to foam. In the first patent, clays were mixed to propellants (calcium carbide, calcium hydroxide, aluminum sulfate, hydrogen peroxide). In acid media, metal blowing agents, like magnesium, calcium, chromium, manganese, iron and cobalt, should be added for promoting hydrogen gas evolution; in alkali media, aluminum is typically employed.

Also in this case a drying and sintering step needs to develop a self-supporting ceramic network.

A foaming agent, as silica gel, carbon black, talc, mica, is often added to give uniform foaming. But, more easily, freon has been dispersed as fine droplets in the slurry, and a surfactant agent disperses the freon and stabilized the gas bubbles. A similar result can be also achieved when a sponge polymeric network is produced simultaneously with the foaming of a ceramic-filled slurry.

Compared to the polymeric sponge method, the foaming method allows to produce small-pore-sized closed-cell foams, which cannot be made by an impregnation technique.

Using this method, Boumchedda[23] developed a porous PZT material for hybrid pressure sensors. In this case an adequate organic additive, which induces an expansion at low temperature in the green body, was choosen: this allows the obtention of highly porous ceramics, having typically 60% open porosity and upper values of about 90%, and a pore size ranging between 0·01 and 1 mm. The ceramic powder presented a particle size distribution close to 1·5 micron; the additive showed a mean particle size of about 20 microns.

A wet mixing of the pore foaming agent with the ceramic powder was performed in ethylic alcohol, being the organic additive insoluble in this medium. After oven drying, the mixture was 100 μm sieve granulated and uniaxially pressed under 100 MPa. At this step the microstructure is only constituted by organic particles well dispersed with the ceramic grains. Then a specific thermal treatment is realized in order to transform the organic additive into a high viscosity liquid which

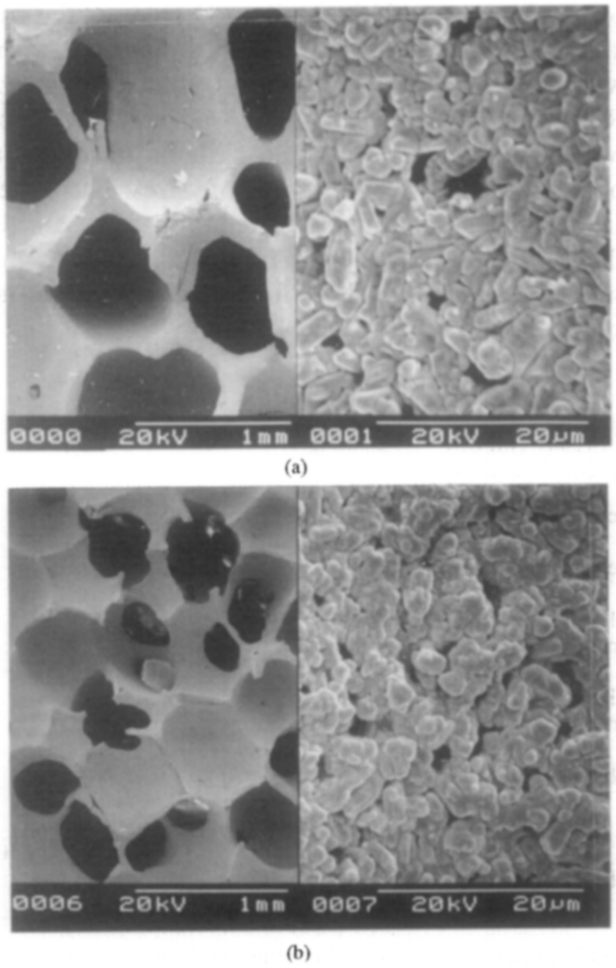

Fig. 6. SEM micrography of struts and pore wall of a ceramic foam: (a) 61 ppi; (b) 32 ppi.

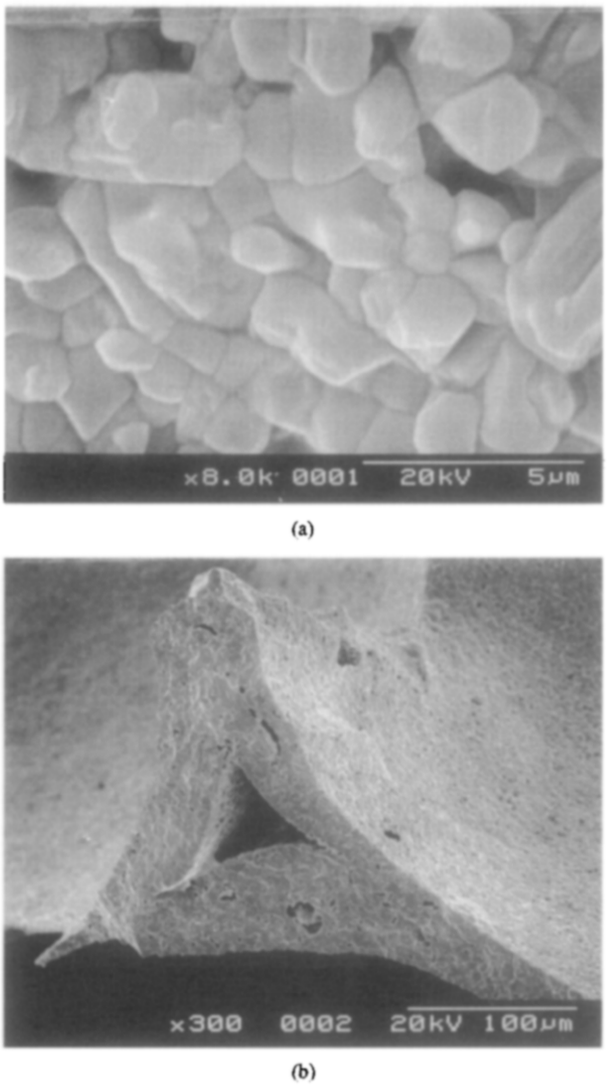

Fig. 7. Micropores and macro defects (triangular voids) of a mullite foam.

surrounds the ceramic particles. The green microstructure in an expanded state was obtained as a result of the decomposition gas pressure and the easiness of the green microstructure deformation.

An illustration of mechanism of transition from the initial green microstructure to the expanded one is given in Fig. 9.

The organic additive (from glucide family) during the thermal treatment must develop a liquid having a sufficiently high viscosity so that the shape of the green body is maintained, no significant deformations appear and no cracks are generated by the gas bubble formation during its decomposition. Moreover, when the temperature is lowered, the remaining organic additive acts as a binder.

Typical microstructures of foams obtained by this method are given in Fig. 10: the sintered density of the resulting ceramic foams was lower than 1 g cm^{-3}, even if the theoretical density of the PZT

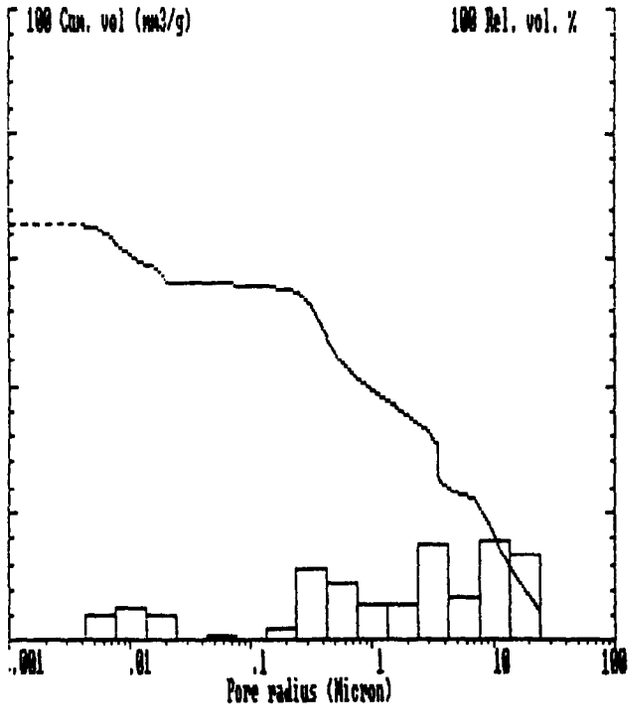

Fig. 8. Pore size distribution of a mullite foam.

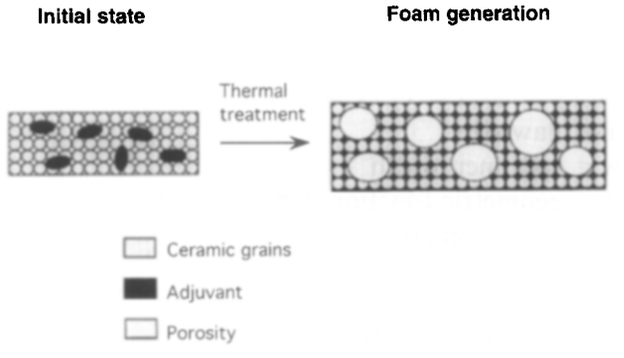

Fig. 9. Scheme of the transition from the initial green microstructure to the green foam microstructure.

is about 7·7 g cm^{-3}. Concerning the microstructure of the wall cell, it can be seen in Fig. 11(a) that a good densification can be obtained with this method. A typical defect observed is given

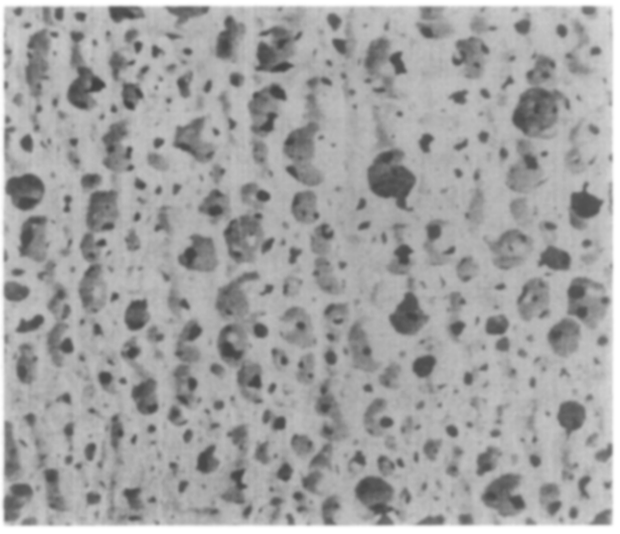

Fig. 10. Typical ceramic foam microstructure obtained by the pore generation method (optical microscope, × 15).

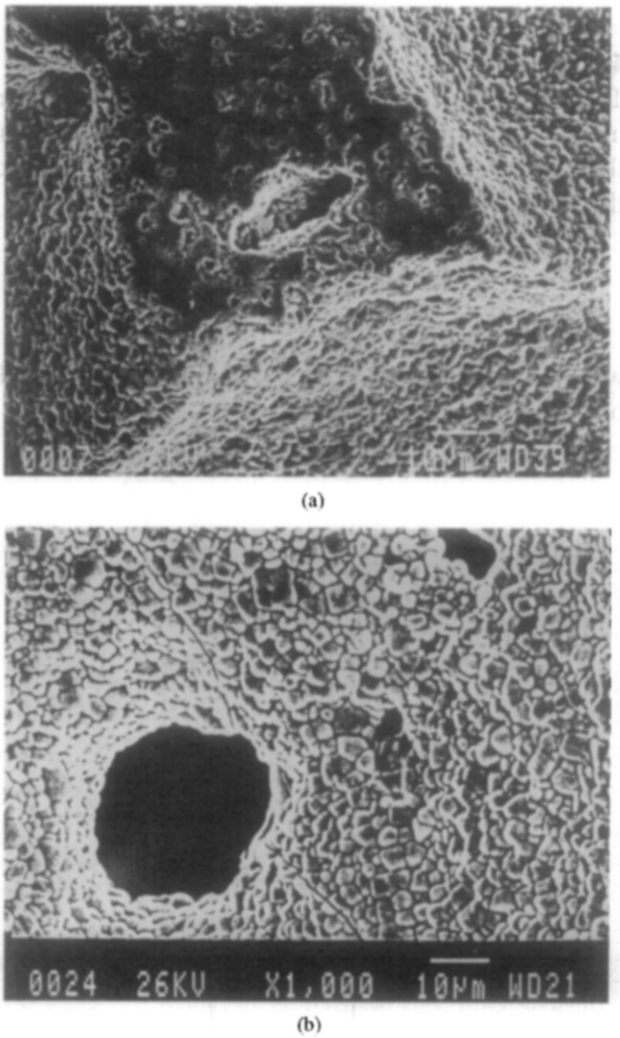

(a)

(b)

Fig. 11. Micropores and macro defects of a P.Z.T. foam obtained by pore generation: (a) aspect of the microstructure in the cell walls; (b) crack defect.

Fig. 11(b). These cracks appear during the sintering process, but they result from residual thermal stresses induced during an inadequate foaming thermal treatment.

4 Mechanical Behaviour of Ceramic Foams

It is important to relate the mechanical behaviour to their microstructure and to know the significant parameters which control this mechanical behaviour.

In order to derive mechanical relationships for cellular ceramics, Gibson and Ashby[24] have proposed an idealized unit cell shown in Fig. 12. A significant property of the foam is the relative density (ρ/ρ_s, where ρ is the density of the bulk foam and ρ_s is the density of the cell edges and faces). The relative density of an open foam is linked to the thickness t of the cell edges or faces, the length L of the edges as follows[2] (for low density):

$$\rho/\rho s = C_1(t/L)^2 \qquad (1)$$

4.1 Elastic behaviour

The cell edge bending is the essential deformation mode of an open foam. By using standard beam theory, the deflection of the cell edges and therefore the elastic modulus can be determined:

$$E/E_s = C_2(t/L)^4 = C_3(\rho/\rho_s)^2 \qquad (2)$$

where E and E_s are, respectively, Young's moduli of the foam and the edge.

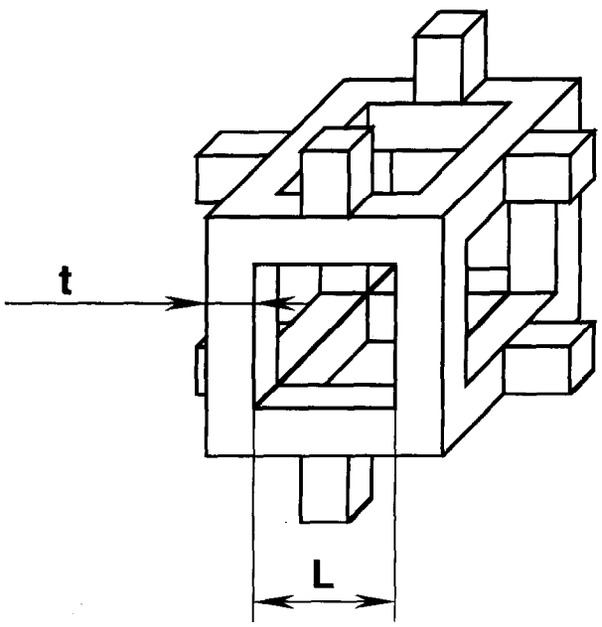

Fig. 12. Scheme of an idealized unit cell (from Ref. 23).

Moreover, foams can show some elastic anisotropy. Experimental data exhibit good agreement with eqn (2) with a C_3 value between 0·36 and 0·5.[2]

An example of dependence of E with the relative density is shown in Fig. 13 for two mullite foams[25] with 32 and 61 p.p.i., respectively. The exponent is near the theoretical one (2) for the 32 p.p.i. foam (1·8) whereas it is higher (2·4) for the 64 p.p.i. foams. This difference is probably due to the fact that the foams are not constituted of totally open cells, but of partially closed cells. In this case, the dependence of E with the relative density is no more given by eqn (2) but by more complex equation.[24]

4.2 Fracture toughness

The fracture toughness of open cell foams depends on the edge strength (σ_{fs}, cell size (L) and relative density as follows:[26]

$$K_{IC} = C_a\sigma_{fs}\sqrt{\pi L}(\rho/\rho s)^{3/2} \qquad (3)$$

with $C_4 \approx 0{\cdot}65$.

In order to optimize the foam toughness, a large cell foam with a high edge strength must be used. So the process must be improved that strut defects (pores, cracks...) may be removed thereby increasing σ_{fs}. Triangular cavity appears during polymer removal in foams obtained by coating and burnout of polymer foams (Fig. 7). The pores as well as other microstructural defects like inclusions or cracks influence the strut strength.

Fracture toughness of brittle foams can be measured either by using the single edge-notched beam geometry[2] or from the work of fracture γ'_f obtained by measuring the area U under the curve load-displacement up to the maximum load.[27] The critical potential energy release rates of the foam G_{IC} is given by:[5]

$$G_{IC} = 2\gamma'_f/p \qquad (4)$$

with $p = \phi/(1-x)$, $x = a/w$
a = flaw size
w = specimen width
π = geometric fonction depending on x and specimen geometry
γ'_f = work of fracture = U pl m^{-1}
m = specimen mass
l = specimen length

Fracture toughness is obtained by the relationship

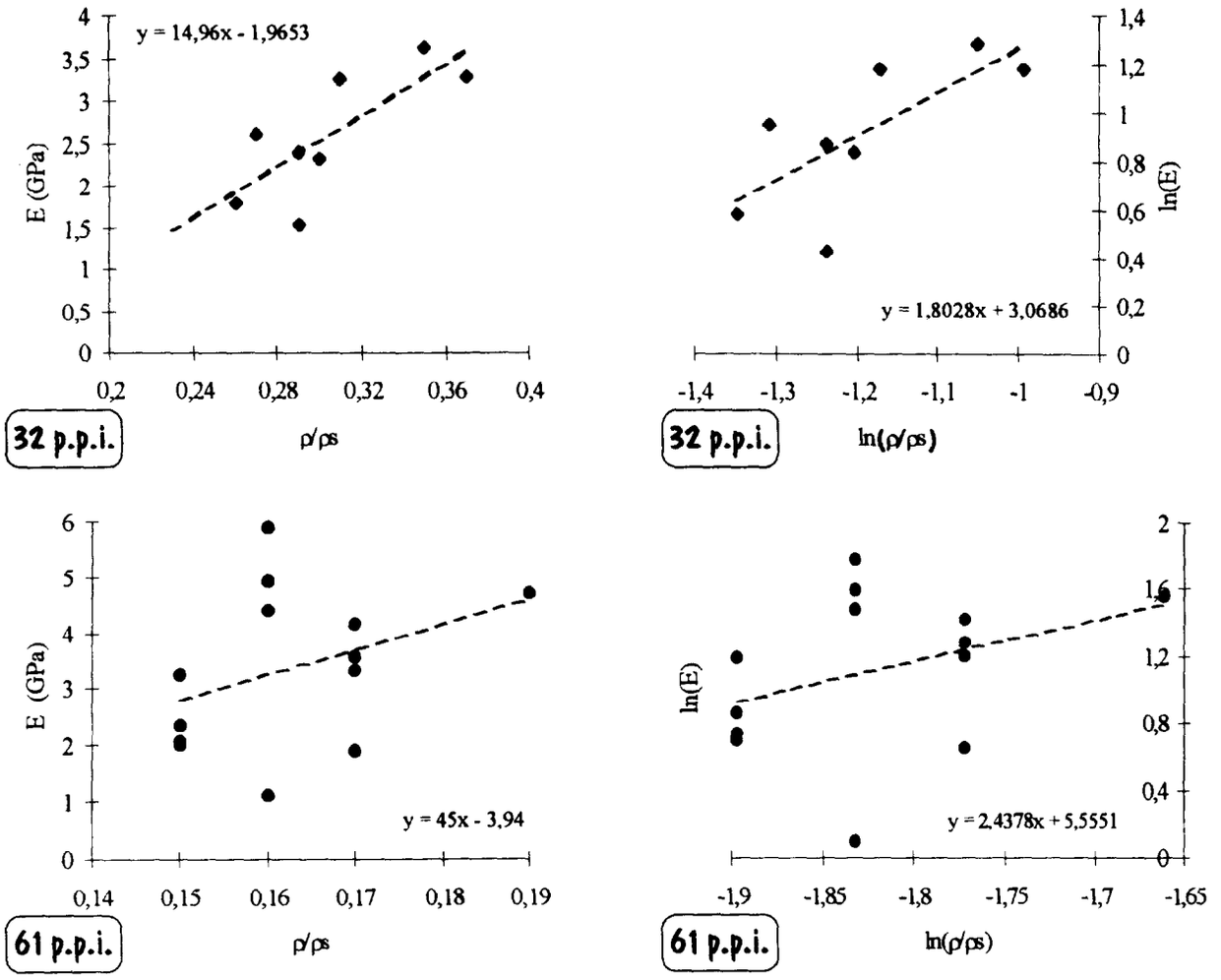

Fig. 13. Example of dependence of E with the relative density (from Ref. 25).

$$K_{IC} = \sqrt{EG_{IC}}$$

The evolution of K_{IC} as a function of relative density for two mullite foams is show in Fig. 14.[25] The fracture toughness increases with relative density for the 32 p.p.i. foam whereas it seems independent for the 61 p.p.i. foam.

This type of plot does not take into account an evolution of the strut strength with density as indicated by eqn (3). From eqns (1) and (3), it can be shown that K_{IC} should increase as $(t/L)^3$. Brezny and Green[28] have measured the strut strength by using the mirror method. They have normalized the fracture toughness with the strut strength and cell size and then plotted this normalized K_{IC} as a function of t/L (Fig. 15). This plot is independent of the relative density as shown by eqn (1). The slope obtained for the alumina-mullite open foam is in good agreement with the Gibson and Ashby model,[24] the slope being near 3.

The two other materials exhibit a more rapid increase, others factors contributing to this increase. Finally, for open cell foams, the fracture toughness can be predicted correctly by eqn (3).

4.3 Tensile strength[2]

Under tensile stress, the struts parallel to the load direction should fail first and should be responsible for the foam strength. In fact, struts are randomly oriented and so failure of struts occurs essentially by bending.

Tensile strength of foams can be obtained by a fracture mechanics approach. Taking into account eqn (3), the tensile strength σ_{ft} is given by the relation:

$$\sigma_{ft} = K_{IC}/\sqrt{a} = C_5\sigma_{fs}\left(\frac{L}{a}\right)^{1/2}\left(\frac{\rho}{\rho s}\right)^{3/2} \qquad (5)$$

C_5 = geometric factor $\cong$ 0·18
a = critical flaw size

For a cellular structure, the lower limit of a is the cell size L.

Equation (5) shows that, for a given density, tensile strength increase requires an improvement in the strut strength σ_{fs}.

The bend strength of two mullite foams have been measured as a function of relative density by

Tulliani in three point bending.[25] The Weibull moduli were estimated from the bend strength results: 1·8 for the 32 p.p.i. foam and 3·2 for the 61 p.p.i. foam. These values are very low, indicating a wide distribution of flaw sizes.

The effect of density on the bend strength of these two mullite foams is shown in Fig. 16. One can notice that bend strength has approximatively a linear dependence on relative density, the dependence being stronger for the 32 p.p.i. foam than for the 61 p.p.i. one. So, the mullite foams do not exhibit a good agreement with eqn (5) and this disagreement can be due to the influence of cell faces, the foams being partially closed.

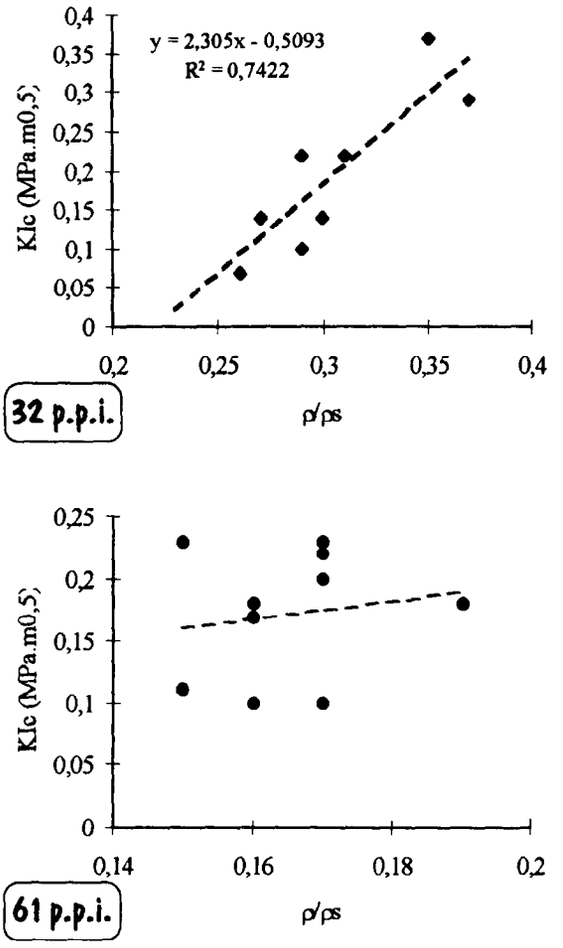

Fig. 14. Example of dependence of K_{IC} with the relative density (from Ref. 25).

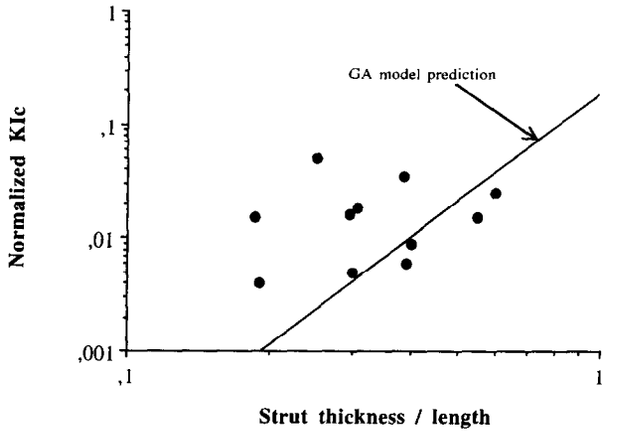

Fig. 15. Dependence of normalized K_{IC} with the t/L ratio. Experimental data for alumina, alumina–zirconia, alumina–mullite and theoretical line given by the G A model (from Ref. 2).

4.4 Compressive strength

Maiti *et al.*[26] have extended the model of Gibson and Ashby to the compressive behaviour of foams. Compressive rupture occurs by struts bending. For open cell ceramics, the compressive strength is given by:

$$\sigma_{fc} = C_6 \sigma_{fs} \left(\frac{\rho}{\rho s}\right)^{3/2} \qquad (6)$$

with $C_6 \cong 0{\cdot}65$. Eqn (6) has the same form as that for tensile strength [eqn (5)] and thus for foams the tensile and compressive strengths are similar. This result is very different from the dense ceramics one (the compressive strength of dense ceramics is an order of magnitude higher than the tensile one).

A typical load-displacement plot of a 61 p.p.i. mullite foam is shown in Fig. 17. An inital linear elastic behaviour is first observed with some strut

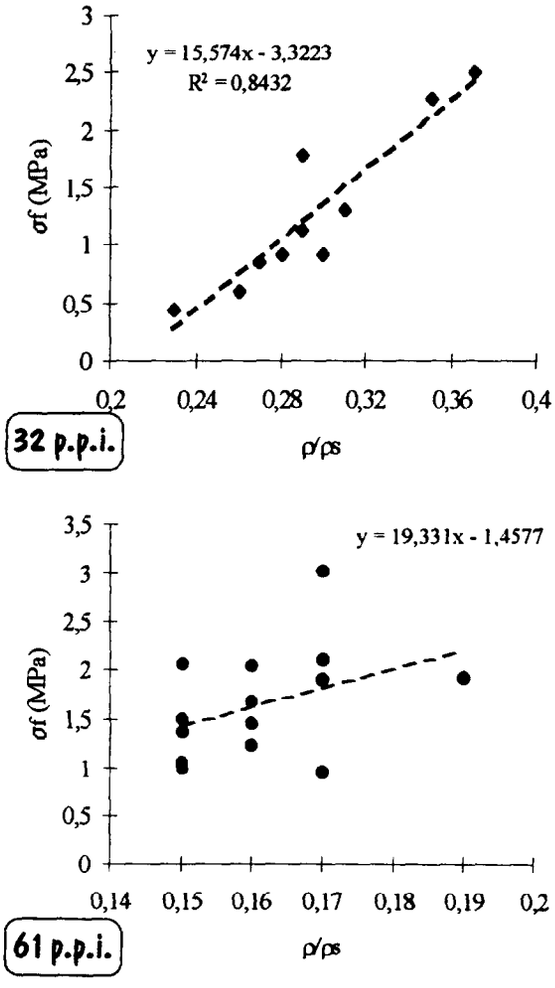

Fig. 16. Example of dependence of the flexural strength with the relative density (from Ref. 25).

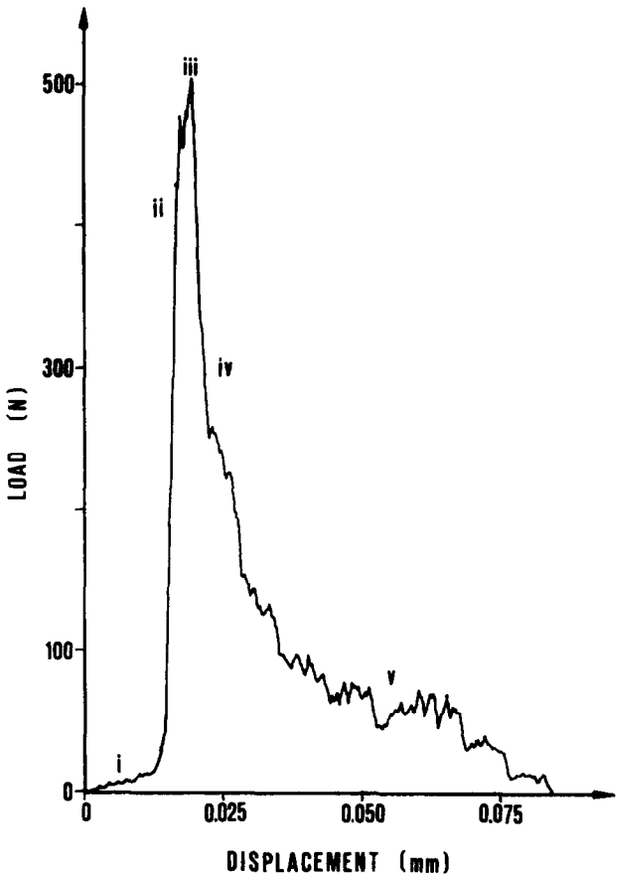

Fig. 17. Typical load—displacement plot (from Ref. 25).

fractures which correspond to slight drops in the stress–strain curve. The stress increases as the damage. At the maximum load, macroscopic cracks propagate with a strong load drop. Finally, densification can occur corresponding to a load increase (not shown in Fig. 17).

Figure 18 shows the variation of compressive strength of mullite foams as a function of relative density.[25] The Weibull moduli are very low as for bend strengths: 2 for the 32 p.p.i. foam and 3·5 for the 61 p.p.i foam.

The compressive strength is higher than bend strength. There is a discrepancy between the experimental results and that predicted by eqn (6). The exponent is about 2 for the 61 p.p.i. foam and 0·3 for the 32 p.p.i. foam.

One reason for this disagreement between theory and experiment can be due to the difficulty to obtain an uniform loading. Another reason is due to the presence of faces (the foams are partially closed cell ceramics) The work of fracture measured during compression is an order of magnitude higher than for tension, due to the cells collapse.

Concerning high temperature behaviour, it is important to know the thermomechanical properties of foams, particularly thermal shock resistance and creep behaviour. Foams presenting low thermal conductivity and toughness, they can be significantly damaged during thermal shock. This

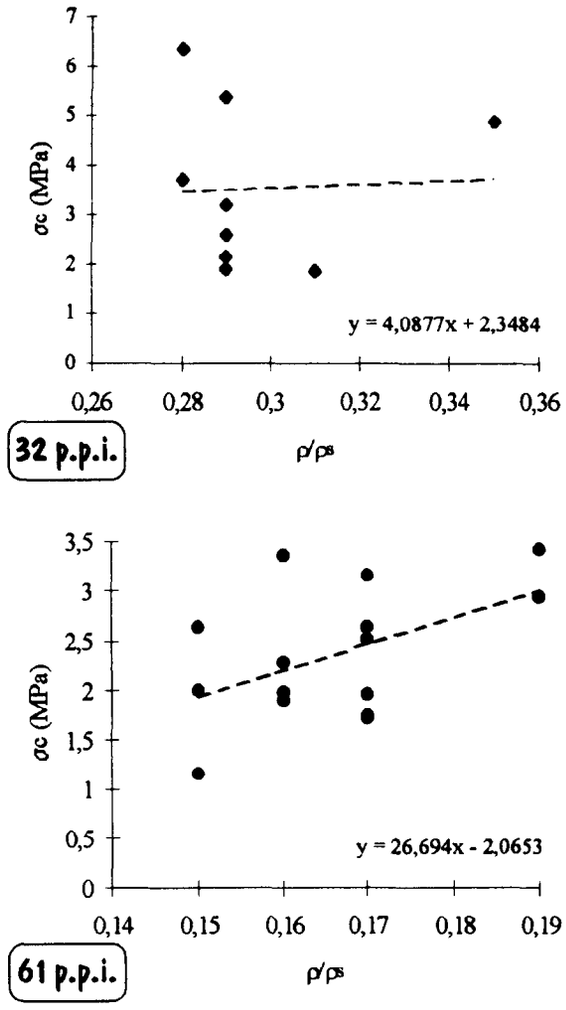

Fig. 18. Example of dependence of the compressive strength with the relative density (from Ref. 25).

thermal shock resistance can be measured by following the elastic modulus, the bend or compressive strength as function of the quenching temperature.[2] Creep and thermal shock behaviour are two important properties for the lifetime of foams.

5 Conclusions

Ceramic foams have an important potential of development, essentially due to the emergence of environmental preoccupations. Nethertheless many others applications may emerge in the near future.

Many elaboration routes have been developed to produce ceramic foams, but it is important to note that, in consideration to the field of the applications previously cited, low cost processes and raw materials are imperatively required. The two examples detailed here are adapted to an industrial production of low cost ceramic filters.

Considering the mechanical properties evaluation of the cellular materials, one can note that numerous studies also exist. On the other hand, little work has been done in the field of the high

temperature corrosion. However, it is clear that in the case of hot filtration, each application will constitute a particular case. So investigations in this field have to be developed.

References

1. Ashby, M. F., The mechanical properties of cellular solids. *Metallurgical Trans. A*, 1983, **14A**, 1755–1769.
2. Brezny, R. and Green, D. J., Mechanical behavior of cellular solids. In *Materials Science and Technology, Vol. 11, Structure and Properties of Ceramics*, ed. R. W. Cahn, P. Haasen and E. J. Kramer. VCH, Germany, 1992, pp. 467–516.
3. Saggio-Woyansky, J., Scott, C. E. and Minnear, W. P., Processing of porous ceramics. *Amer. Cer. Soc. Bull.*, 1992, **71**(11), 1674–1682.
4. Inui, T. and Otowa, T., Catalytic combustion of benzene-soot captured on ceramic foam matrix. *Appl. Catalysis*, 1985, **14**, 83–93 .
5. Masuda, T., Tomita, K. and Iwata, T., Application of ceramic foam. In *Ceramic Transactions, Vol. 31, Porous Materials*, ed. Ishizaki *et al.* The American Ceramic Society, Westerville, OH, 1993, pp. 285–293.
6. Mizrah., T., Maurer, A., Gauckler, L. and Gabathuler, J. P., Open-pore ceramic foam as Diesel particulate filter. SAE Paper 890172, 1989.
7. Tulliani, J. M., Montanaro, L. and Borello, C., Open-pore mullite foams for Diesel particulate filtration. Proceedings of the 4th Euroceramics, Vol. 4, Basic Science-Trends in Emerging Materials and Applications, ed. A. Bellosi. Faenza Editrice, Faenza, Italy 1995, pp. 493–500.
8. Ceramic foams for molten-metal filtration. *Amer. Cer. Soc. Bull.*, 1991, **70**(7), 1149–1150.
9. Otzuka, M. and Akiyama, T., Structure and mechanical behavior of ceramic foams. In Ceramic: Charting the Future, ed. Vincenzini. Techna, Italy, 1995, pp. 2431–2438.
10. Tutko, J. J., Lestz, S. S., Brockmeyer, J. W. and Dore, J. E., Feasibility of ceramic foam as a Diesel particulate trap. SAE Paper 840073, 1984.
11. Tantry, P. K., Misra, S. N. and Shashi Mohan, A. L., Developmental studies on porous alumina ceramics. In *Ceramic Transactions, Vol. 31, Porous Materials*, ed. Ishizaki *et al.* The American Ceramic Society, Westerville, OH, 1993, pp. 89–99.
12. Lange, F. F. and Miller, K. T., Open-cell, low-density ceramics fabricated from reticulated polymer substrates. *Adv. Ceram. Mater.*, 1987, **2**(4), 827–831.
13. Lannguth, K., Preparation of macro-porous SiC–Al_2O_3 composites with polysilanes and polycarbosilanes. *Ceram. Intern.*, 1995, **21**, 237–242.
14. Sherman, A. J., Tuffias, R. H. and Kaplan, R. B., Refractory ceramic foams: a novel, new high-temperature structure. *Amer. Cer. Soc. Bull*, 1991, **70**(6), 1025–1029.
15. Sheppard, L. M., Porous ceramics: processing and applications. In *Ceramic Transactions, Vol. 31, Porous Materials*, ed. Ishizaki *et al.* The American Ceramic Society, Westerville, OH, 1993, pp. 3–25.
16. White, L. R., Tompkins, T. L., Hsieh, K. C. and Johnson, D. D., Ceramic filters for gas cleanup. *J. Engin. for gas turbines and power*, 1993, **115**(7), 665–669.
17. Alvin, M. A., Lippert, T. E. and Lane, J. E., Assessment of porous ceramic materials for hot gas filtration applications. *Amer. Cer. Soc. Bull*, 1991, **70**(9), 1491–1498.
18. Gabathuler, J. P., Mizrah, T., Dole, M. and Bressler, H., Filter for cleaning exhaust gases of Diesel engines. US Patent no. 4913712, 1990.
19. Schwartzwalder, K. and Somers, A. V., Method of making porous ceramic articles. US Patent no. 3 090 094, 1963.
20. Chou, K. S., Liu, H. C. and Chang, K. L., Microstructure evolution during fabrication of a porous ceramic filter. In *Ceramic Transactions, Vol. 31, Porous Materials*, ed. Ishizaki *et al.* The American Ceramic Society, Westerville, OH, 1993, pp. 101–110.
21. Tulliani, J. M., Montanaro, L., Swain, M. V. and Bell, T., Semi-closed cell mullite foams. Submitted to *J.A.C.S.*
22. Sundermann, E. and Viedt, J., Method of manufacturing ceramic foam bodies. US Pat no. 3 745 201, 1973.
23. Boumchedda, K., Elaboration and characterization of composite piezoelectric materials of 3–3 connection. Ph.D. thesis, INSA, Lyon, France, 1994.
24. Gibson, L. J. and Ashby, M. F., *Cellular Solids: Structure and Properties*. Pergamon Press, New York, 1988.
25. Tulliani, J. M., Ph.D. thesis.
26. Maiti, S. K., Ashby, M. F. and Gibson, L. S., *Scripta. Metall.*, 1984, **18**, 213-217.
27. Fantozzi, G., *Fracture of Materials*. Institut National des Sciences Appliquées de Lyon, France, 1996.
28. Brezny, R. and Green, D. J., *J. Am. Ceram. Soc.*, 1989, **72**, 1145–1152.